Pak.j.stat.oper.res. Vol.22 No.3 2026 pp 433-458 DOI: http://dx.doi.org/10.18187/pjsor.v22i3.4923

Pakistan Journal of Statistics and Operation Research

A Wrapped New Polynomial One-Parameter Distribution with Applications to Ecological and Wind Direction Data

Swapnil Swagat Phookan[1], Partha Jyoti Hazarika[2], Sajadul Hussain[3], G. G. Hamedani[4*]

*Corresponding author

1. Department of Statistics, Dibrugarh University, Assam, India, swapnilswagatphukon@gmail.com
2. Department of Statistics, Dibrugarh University, Assam, India, parthajhazarika@gmail.com
3. Department of Statistics, Dibrugarh University, Assam, India, sajadul.hussain122@gmail.com
4. Department of Mathematical and Statistical Sciences, Marquette University, USA, gholamhoss.hamedani@marquette.edu

Abstract

Observations recorded as angles or directions appear across a wide range of scientific fields, from ecology and environmental to atmospheric science and materials research. Because such circular data follow a periodic structure, standard statistical tools fail to capture their geometry, and purpose-built circular distributions are required. This study proposes the Wrapped New Polynomial Single-Parameter (WNPS) distribution, a novel one-parameter circular model constructed by wrapping the New Polynomial Single-Parameter distribution onto the unit circle. A systematic study of its mathematical structure gives the closed-form expressions for the survival function, hazard rate, modality conditions, characteristic function, trigonometric moments,invariance behavior and Rényi entropy measures. Also, various characterizations of the proposed distribution are presented. Parameter estimation is addressed through ten frequentist procedures alongside a Bayesian framework employing five loss functions from both symmetric and asymmetric penalization. Monte Carlo simulation experiment compares the finite-sample behavior of all estimators across varying sample sizes and parameter configurations. The usefulness of the WNPS distribution in practice is illustrated via two real-life datasets consisting of angular measurements from an ecological study and another on wind direction. Goodness-of-fit comparisons against the wrapped Lindley, wrapped modified Lindley, wrapped XLindley, and related competitors confirm the WNPS distribution as a competitive and parsimonious choice for circular data modeling.

Key Words: Wrapped distribution; Trigonometric moments; Invariance Behavior; Loss functions; Monte Carlo simulation; Wind Directional data.

Mathematical Subject Classification: 60E05, 62E15.

1. Introduction

The analysis of directional phenomena has attracted considerable attention in recent years due to its wide range of applications in science and engineering. Observations recorded as angles or directions exhibit a circular nature, where 0° and 360° correspond to the same point, making conventional linear statistical methods unsuitable for their analysis (Fisher, 1995; Mardia and Jupp, 2009). Such data commonly arise in meteorology, oceanography, biology, geology, navigation, and time-related studies (Jammalamadaka and Sengupta, 2001). To model these observations effectively, a variety of circular probability distributions have been developed. However, many real-world datasets display characteristics such as asymmetry, multimodality, and varying degrees of concentration that are not adequately represented by existing models. Therefore, the development of new circular probability distributions continues to be an active and important area of research, offering greater flexibility and improved modeling of complex directional data.

The wrapping technique is a classical and widely adopted method for generating circular distributions from linear distributions. The basic idea is to wrap the real line around the circumference of a unit circle by taking observations modulo 2π. This approach was formalized in the pioneering work of (Mardia and Jupp, 2009) on directional statistics. Specifically, if X is a continuous random variable with probability density function $f(x), x \in R$, then the circular random variable $Y = X(\text{mod } 2\pi)$ is called the wrapped version of X. The probability density function of Y is given by

$$g(y) = \sum_{k=0}^{\infty} f(y + 2\pi k), \;\; y \in [0, 2\pi)$$

Over the years, a substantial body of research has emerged on wrapped distributions, resulting in the introduction of several important circular models, including the Wrapped Normal (Nagano et al., 2019), Wrapped Cauchy (Kato and Jones, 2013), Wrapped Exponential (Yilmaz and Biçer, 2018), Wrapped Lindley (Joshi and Jose, 2018), Wrapped XLindley (Zinhom et al., 2023), Wrapped Modified Lindley (Chesneau et al., 2021), Wrapped Two-Parameter Lindley (Bhattacharjee et al., 2021), Wrapped new XLindley (Gemeay and Abd El-Bar, 2026), Wrapped Xgamma (Al-Mofleh and Sen, 2019), and Wrapped Akash distributions (Al-Meanazel and Al-Khazaleh, 2021), as well as numerous extensions thereof. The growing number of such distributions reflects the increasing need for flexible and robust circular models capable of accommodating the complexities of directional data. Consequently, the development of new wrapped distributions continues to play a vital role in enhancing the modeling of real-world circular phenomena across a wide range of scientific applications.

The New Polynomial Single-Parameter (NPS) distribution, proposed by (Keddali et al., 2026), has attracted attention due to its flexibility and tractable mathematical properties. The corresponding probability density function (pdf) and cumulative distribution function (cdf) are given, respectively, by

$$F(x) = 1 - \left(1 + \omega^2 x^2\right) e^{-2\omega x}, \qquad x > 0, \; \omega > 0$$

and

$$f(x) = 2\omega \left(\omega^2 x^2 - \omega x + 1\right) e^{-2\omega x}, \qquad x > 0, \; \omega > 0$$

Recognizing the absence of a wrapped analogue of the New Polynomial Single-Parameter (NPS) distribution in the existing body of literature, this study proposes the Wrapped New Polynomial Single-Parameter (WNPS) distribution. The WNPS distribution is a novel one-parameter circular model constructed by applying the wrapping technique to the NPS distribution on the unit circle. The proposed WNPS distribution is studied in detail by examining its fundamental statistical properties, including the characteristic function, trigonometric moments, invariance properties, Rényi entropy and characterizations. Model parameter estimation is carried out using ten classical and Bayesian estimation techniques, and their performance is evaluated through a comprehensive simulation study. Furthermore, the practical utility of the proposed model is illustrated using two real-world directional datasets from biological and meteorological applications. Comparative analyses reveal that the WNPS distribution provides a superior fit relative to several well-established wrapped distributions.

The rest of the paper is organized as follows. Section 2 presents the proposed WNPS distribution, and Section 3 derives its main statistical properties. Parameter estimation procedures are discussed in Section 4, followed by a comprehensive simulation study in Section 5. Section 6 illustrates the usefulness of the proposed model through applications to two real-world directional datasets. Finally, Section 7 concludes the paper.

2. The Proposed Wrapped Distribution

In the present section, we introduce the probability density function (pdf) and cumulative distribution function (cdf) of the proposed WNPS distribution and investigate its behavior for various parameter configurations using graphical illustrations. We begin with the definition of the proposed WNPS distribution, which serves as the foundation for the subsequent theoretical developments.

Definition 1 Let X be a random variable following the NPS distribution with parameter ω, i.e., $X \sim \text{NPSD}(\omega)$. Then, the wrapped random variable $Y = X(\text{mod } 2\pi)$ follows the WNPS distribution with probability density function given by

$$\begin{aligned} g(y;\omega) &= \sum_{k=0}^{\infty} f(y+2k\pi) \\ &= 2\omega e^{-2\omega y}\varrho_0^{-3}\left[(\omega^2y^2-\omega y+1)\varrho_0^2+(4\pi\omega^2 y-2\pi\omega)e^{-4\pi\omega}\varrho_0+4\pi^2\omega^2 e^{-4\pi\omega}\varrho_1\right], \quad 0 \le y < 2\pi,\ \omega > 0. \end{aligned} \tag{1}$$

Where, $\varrho_0 = 1-e^{-4\pi\omega}$, and $\varrho_1 = 1+e^{-4\pi\omega}$.

Definition 2 Let $Y \sim$ WNPSD(ω). Then, the cumulative distribution function (cdf) of Y is given by

$$\begin{aligned} G(y;\omega) &= \sum_{k=0}^{\infty}\left[F(y+2k\pi)-F(2k\pi)\right] \\ &= \varrho_0^{-3}\left[(1-e^{-2\omega y}(1+\omega^2y^2))\varrho_0^2-4\omega^2\pi e^{-4\pi\omega}\{y\varrho_0 e^{-2\omega y}-\pi\varrho_1\left(1-e^{-2\omega y}\right)\}\right] \end{aligned} \tag{2}$$

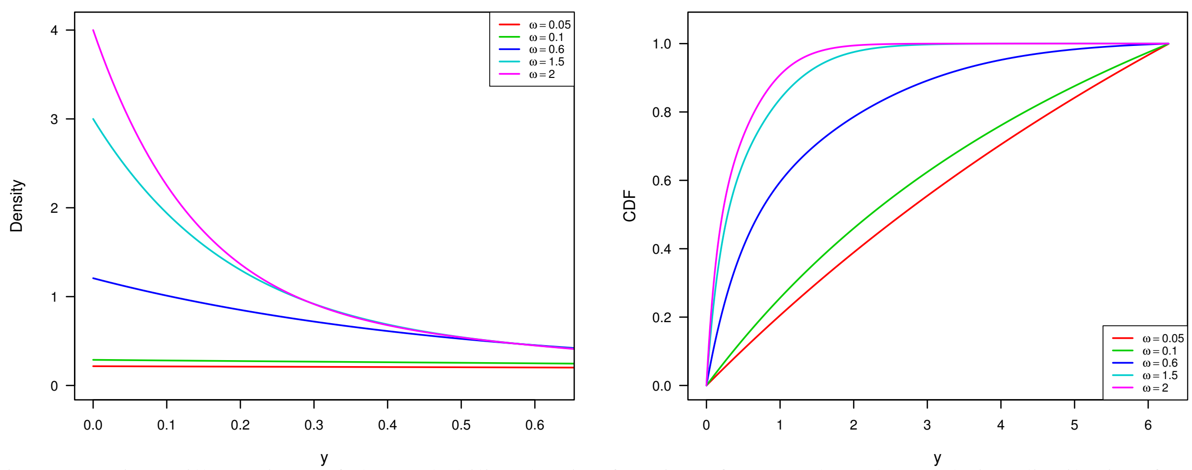

Figure 1: Linear illustrations of the probability density function (first panel) and cumulative distribution function (second panel) of the WNPS distribution for selected values of ω

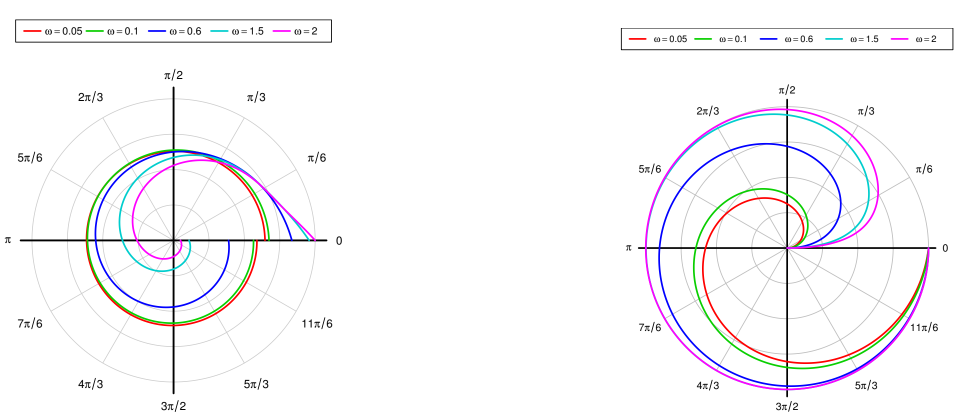

Figure 2: Circular illustrations of the probability density function (first panel) and cumulative distribution function (second panel) of the WNPS distribution for selected values of ω

The graphical behavior of the proposed WNPS distribution for selected values of ω is illustrated through the linear

and circular plots presented in Figures 1 and 2, respectively. With increasing ω, the density exhibits a more prominent J-shaped profile and the CDF becomes increasingly concave, indicating a higher concentration of probability mass near (y=0). These observations demonstrate the ability of the WNPS model to capture a wide range of concentration patterns on the circular domain.
Furthermore, the circular representation highlights the flexibility of the WNPS model in capturing a broad spectrum of concentration patterns over the circular domain.

3. Theoretical Properties of the WNPS Distribution

3.1. Survival and Hazard Rate Functions

The survival function and the corresponding hazard rate function for the WNPS distribution are given, respectively, by

$$S(y;\omega) = \varrho_0^{-3}\left[e^{-2\omega y}A_2(y) - e^{-4\pi\omega}A(0)\right]$$

and

$$h(y;\omega) = \frac{2\omega e^{-2\omega y}A_1(y)}{e^{-2\omega y}A_2(y) - e^{-4\pi\omega}A(0)} \tag{3}$$

Wehre, $A(0) = \varrho_0^2 + 4\omega^2\pi^2\varrho_1$, $A_1(y) = (\omega^2y^2 - \omega y + 1)\varrho_0^2 + (4\pi\omega^2 y - 2\pi\omega)e^{-4\pi\omega}\varrho_0 + 4\pi^2\omega^2 e^{-4\pi\omega}\varrho_1$,

and $A_2(y) = \varrho_0^2(1+\omega^2y^2) + 4\omega^2\pi e^{-4\pi\omega}(y\varrho_0 + \pi\varrho_1)$.

3.2. Asymptotic and Differential Properties of the WNPS Distribution

The asymptotic behavior of the probability density function (pdf) of the WNPS distribution at the boundary points 0 and 2π are given by the following expressions, respectively:

$$2\omega\varrho_0^{-3}\left[\varrho_0^2 - 2\pi\omega e^{-4\pi\omega}\varrho_0 + 4\pi^2\omega^2 e^{-4\pi\omega}\varrho_1\right]$$

and

$$2\omega e^{-4\pi\omega}\varrho_0^{-3}\left[(4\pi^2\omega^2 - 2\pi\omega + 1) + (4\pi^2\omega^2 + 2\pi\omega - 2)e^{-4\pi\omega} + e^{-8\pi\omega}\right]$$

It is observed that the hazard rate function defined in equation (3) diverges to $+\infty$ as $y \to 2\pi^-$. On the other hand, its limiting value as $y \to 0^+$ is given by

$$2\omega\varrho_0^{-3}\left[1 + (4\pi^2\omega^2 - 2\pi\omega - 2)e^{-4\pi\omega} + (4\pi^2\omega^2 + 2\pi\omega + 1)e^{-8\pi\omega}\right]$$

To examine the shape characteristics of the WNPS distribution, the first and second-order derivatives of its probability density function with respect to y are obtained as follows:

$$g^{'}(y) = -2\omega^2 e^{-2\omega y}\varrho_0^{-3}\left[(2\omega^2y^2 - 4\omega y + 3)\varrho_0^2 + 8\pi\omega(\omega y - 1)e^{-4\pi\omega}\varrho_0 + 8\pi^2\omega^2 e^{-4\pi\omega}\varrho_1\right] \tag{4}$$

and

$$g^{''}(y) = 4\omega^3 e^{-2\omega y}\varrho_0^{-3}\left[\varrho_0^2(2\omega^2y^2 - 6\omega y + 5) + 4\pi\omega(2\omega y - 3)e^{-4\pi\omega}\varrho_0 + 8\pi^2\omega^2 e^{-4\pi\omega}\varrho_1\right] \tag{5}$$

3.3. Characteristic Function

Using the methodology introduced by (Jammalamadaka and Sengupta, 2001) for deriving characteristic functions of wrapped distributions, the characteristic function of the WNPS distribution is obtained from its parent distribution and is presented below.

Theorem 3.1. *The characteristic function for the WNPS distribution can be written as*

$$\phi_Y(t) = \frac{2\omega\{(4\omega^2-t^2)^2+9\omega^2t^2\}^{1/2}}{(4\omega^2+t^2)^{3/2}} e^{3i\arctan\left(\frac{t}{2\omega}\right) - i\arctan\left(\frac{3\omega t}{4\omega^2-t^2}\right)}; \;\; i=\sqrt{-1}, \;\; t = \pm1, \pm2, ... \tag{6}$$

Proof Let $\phi_Y(t)$ and $\phi_X(s)$ represent the characteristic functions of the WQL and QL distributions, respectively. Using the relationship for wrapped distributions provided in (Jammalamadaka and Sengupta, 2001), we obtain

$$\phi_Y(t) = \phi_X(t); \ \ t = \pm 1, \pm 2, ...$$

The characteristic function corresponding to the NPS distribution is given by

$$\phi_X(s) = \frac{2\omega(4\omega^2 - s^2 - 3i\omega s)}{(2\omega - is)^3}; \ \ i = \sqrt{-1}$$

Consequently, the characteristic function of the WNPS distribution is obtained as

$$\phi_Y(t) = \frac{2\omega(4\omega^2 - t^2 - 3i\omega t)}{(2\omega - it)^3}; \ \ i = \sqrt{-1}, \ \ t = \pm 1, \pm 2, ... \tag{7}$$

By expressing the complex-valued terms through Euler's representation, equation (7) becomes

$$\phi_Y(t) = \frac{2\omega\{(4\omega^2 - t^2)^2 + 9\omega^2 t^2\}^{1/2}}{(4\omega^2 + t^2)^{3/2}} e^{3i\arctan\left(\frac{t}{2\omega}\right) - i\arctan\left(\frac{3\omega t}{4\omega^2 - t^2}\right)}$$

3.4. Trigonometric Moments and Related Circular Statistics

We present the p^{th} non-central and central trigonometric moments of the WNPS distribution through the following theorem and corollary.

Theorem 3.2. *An explicit expression for the p^{th} non-central trigonometric moment of the WNPS distribution is given by*

$$\alpha_p = \frac{2\omega\{(4\omega^2 - p^2)^2 + 9\omega^2 p^2\}^{1/2}}{(4\omega^2 + p^2)^{3/2}} \cos\left\{3\arctan\left(\frac{p}{2\omega}\right) - \arctan\left(\frac{3\omega p}{4\omega^2 - p^2}\right)\right\} \tag{8}$$

and

$$\beta_p = \frac{2\omega\{(4\omega^2 - p^2)^2 + 9\omega^2 p^2\}^{1/2}}{(4\omega^2 + p^2)^{3/2}} \sin\left\{3\arctan\left(\frac{p}{2\omega}\right) - \arctan\left(\frac{3\omega p}{4\omega^2 - p^2}\right)\right\} \tag{9}$$

Proof By expressing the characteristic function in terms of its real and imaginary components and utilizing the framework of trigonometric moments given in (Jammalamadaka and Sengupta, 2001), equation (7) can be rewritten as

$$\phi_Y(p) = \kappa_p e^{i\mu_p} = \kappa_p(\cos\mu_p + i\sin\mu_p)$$

By equating the above expression with the standard complex form $\alpha_p + i\beta_p$, we obtain

$$\alpha_p = \kappa_p \cos\mu_p \tag{10}$$

$$\beta_p = \kappa_p \sin\mu_p \tag{11}$$

Here, $\kappa_p = \frac{2\omega\{(4\omega^2-p^2)^2+9\omega^2p^2\}^{1/2}}{(4\omega^2+p^2)^{3/2}}$ and $\mu_p = 3\arctan\left(\frac{p}{2\omega}\right) - \arctan\left(\frac{3\omega p}{4\omega^2-p^2}\right)$. Consequently, by combining equations (10) and (11), we obtain

$$\alpha_p = \frac{2\omega\{(4\omega^2 - p^2)^2 + 9\omega^2 p^2\}^{1/2}}{(4\omega^2 + p^2)^{3/2}} \cos\left\{3\arctan\left(\frac{p}{2\omega}\right) - \arctan\left(\frac{3\omega p}{4\omega^2 - p^2}\right)\right\}$$

and

$$\beta_p = \frac{2\omega\{(4\omega^2 - p^2)^2 + 9\omega^2 p^2\}^{1/2}}{(4\omega^2 + p^2)^{3/2}} \sin\left\{3\arctan\left(\frac{p}{2\omega}\right) - \arctan\left(\frac{3\omega p}{4\omega^2 - p^2}\right)\right\}$$

Corollary 1 The p^{th} central trigonometric moment of the WNPS distribution are given by

$$\begin{aligned}\bar{\alpha}_p &= \kappa_p \cos(\mu_p - p\mu_1)\\ &= \frac{2\omega\left\{(4\omega^2-p^2)^2+9\omega^2p^2\right\}^{1/2}}{(4\omega^2+p^2)^{3/2}} \cos\left[\left\{3\arctan\left(\frac{p}{2\omega}\right) - \arctan\left(\frac{3\omega p}{4\omega^2-p^2}\right)\right\} - p\left\{3\arctan\left(\frac{1}{2\omega}\right) - \arctan\left(\frac{3\omega}{4\omega^2-1}\right)\right\}\right]\end{aligned}$$

and

$$\begin{aligned}\bar{\beta}_p &= \kappa_p \sin(\mu_p - p\mu_1)\\ &= \frac{2\omega\left\{(4\omega^2-p^2)^2+9\omega^2p^2\right\}^{1/2}}{(4\omega^2+p^2)^{3/2}} \sin\left[\left\{3\arctan\left(\frac{p}{2\omega}\right) - \arctan\left(\frac{3\omega p}{4\omega^2-p^2}\right)\right\} - p\left\{3\arctan\left(\frac{1}{2\omega}\right) - \arctan\left(\frac{3\omega}{4\omega^2-1}\right)\right\}\right]\end{aligned}$$

3.5. Mean and Associated Statistical Measures

Theorem 3.3. *Explicit expressions for the mean direction, mean resultant length, circular variance, and circular standard deviation of the WNPS model are respectively obtained as*

$$\mu = \mu_1 = 3\arctan\left(\frac{1}{2\omega}\right) - \arctan\left(\frac{3\omega}{4\omega^2-1}\right)$$

$$\kappa = \kappa_1 = \frac{2\omega\{(4\omega^2-1)^2+9\omega^2\}^{1/2}}{(4\omega^2+1)^{3/2}}$$

$$V = 1-\kappa_1 = 1 - \frac{2\omega\{(4\omega^2-1)^2+9\omega^2\}^{1/2}}{(4\omega^2+1)^{3/2}}$$

and

$$\sigma = \sqrt{-2\log\kappa_1} = \sqrt{-2\log\left(\frac{2\omega\{(4\omega^2-1)^2+9\omega^2\}^{1/2}}{(4\omega^2+1)^{3/2}}\right)}$$

Proof Setting $p = 1$ in the expressions for μ_p and κ_p yields the required results.

3.6. Coefficients of Circular Skewness and Kurtosis

The coefficients of circular skewness γ_1 and circular kurtosis γ_2 associated with the WNPS model are respectively given by

$$\begin{aligned}\gamma_1 &= \frac{\bar{\beta}_2}{V^{3/2}}\\ &= \frac{2\omega\{(4\omega^2-4)^2+36\omega^2\}^{1/2}}{(4\omega^2+4)^{3/2}}\left\{1-\frac{2\omega\{(4\omega^2-1)^2+9\omega^2\}^{1/2}}{(4\omega^2+1)^{3/2}}\right\}^{-3/2}\sin(\mu_2-2\mu_1)\end{aligned}$$

and

$$\begin{aligned}\gamma_2 &= \frac{\bar{\alpha}_2-\kappa^4}{V^2}\\ &= \left[\frac{2\omega\{(4\omega^2-4)^2+36\omega^2\}^{1/2}}{(4\omega^2+4)^{3/2}}\cos(\mu_2-2\mu_1) - \frac{16\omega^4\{(4\omega^2-1)^2+9\omega^2\}^2}{(4\omega^2+1)^6}\right]\left(1-\frac{2\omega\{(4\omega^2-1)^2+9\omega^2\}^{1/2}}{(4\omega^2+1)^{3/2}}\right)^{-2}\end{aligned}$$

Table 1 summarizes the numerical values of selected characteristics of the WNPS distribution for various choices of ω. The results reveal a declining pattern in the mean direction, circular variance, circular standard deviation, and circular skewness with increasing ω. In contrast, the mean resultant length and circular kurtosis exhibit a monotonic increase over the same range of parameter values.

Table 1: Numerical Evaluation of the WNPS Distribution Characteristics for Different Values of ω

Distribution Properties		Parameter Configuration(ω)			
		0.05	1.5	5	8
Trigonometric moments					
Non-Cental	α_1	-0.0146	0.7830	0.9756	0.9903
	α_2	-0.0037	0.5039	0.9089	0.9624
	β_1	-0.0976	0.3810	0.1461	0.0928
	β_2	-0.0497	0.4247	0.2705	0.1799
Central	$\bar{\alpha_1}$	0.0986	0.8708	0.9865	0.9947
	$\bar{\alpha_2}$	-0.0110	0.6451	0.9483	0.9790
	$\bar{\beta_1}$	0	0	0	0
	$\bar{\beta_2}$	0.0486	-0.1344	-0.0076	-0.0019
Mean direction	μ	4.5637	0.4529	0.1486	0.0934
Resultant length	κ	0.0986	0.8708	0.9865	0.9947
Circular variance	V	0.9014	0.1292	0.0135	0.0053
Circular standard deviation	σ	2.152	0.5261	0.1651	0.1035
Circular skewness	γ_1	0.0567	-2.8934	-4.7982	-4.9879
Circular kurtosis	γ_2	-0.0136	4.2017	7.3069	7.6210

3.7. Invariance Behavior of WNPS Distribution

Circular data are characterized by arbitrary choices of reference direction and orientation. Therefore, it is essential that any circular model possesses invariance properties with respect to these choices. Models that do not satisfy such invariance properties may lead to incorrect statistical inference and misleading conclusions.
A circular distribution with pdf $g(y;\omega)$ is invariant under changes of origin and orientation if and only if, for every $\theta \in \{-1, 1\}$ and $\epsilon \in [0, 2\pi)$, the transformed variable $Y^* = \theta(Y + \epsilon) \pmod{2\pi}$, has a pdf belonging to the same family as $g(y;\omega)$.(see (Mastrantonio et al., 2019))
The characteristics function of Y^* is given by

$$\begin{aligned}\phi_{Y^*}(t) &= E[e^{ity^*}] \\ &= E[e^{it\theta(y+\epsilon)}] \\ &= e^{it\theta\epsilon}\phi_Y(t) \\ &= \frac{2\omega\left(\cos(t\theta\epsilon) + i\sin(t\theta\epsilon)\right)\left(4\omega^2 - t^2 - 3i\omega t\right)}{(2\omega - it)^3}\end{aligned} \tag{12}$$

Equation 7 can be obtained as a special case of Equation 12 by setting $\theta = 1$ and $\epsilon = 0$. Hence, both circular random variates Y and Y^* belong to the same family of distributions, thereby confirming that the WNPS distribution satisfies the invariance property.

3.8. Rényi Entropy

Entropy provides a quantitative measure of the uncertainty inherent in a probability distribution. Among the various entropy measures available in the literature, Rényi entropy has received considerable attention due to its flexibility and broad applicability. For a circular random variable with probability density function $g(y)$, the Rényi entropy is defined as

$$E_Y(\lambda) = \frac{1}{1-\lambda}\ln\int_0^{2\pi}\{g(y)\}^{\lambda}dy; \quad \lambda > 0, \lambda \neq 1$$

An explicit expression for the Rényi entropy of the WNPS distribution is obtained as follows, where ${}_1F_1$ denotes the confluent hypergeometric function of first kind; see (Abramowitz and Stegun, 1948) for its definition and properties.

$$E_Y(\lambda) = \frac{1}{1-\lambda}\ln\left[\frac{2^{\lambda}\omega^{3\lambda}}{\varrho_0(2\lambda+1)}\left\{\left(2\pi - \frac{1}{2\omega} + \frac{2\pi e^{-4\pi\omega}}{\varrho_0}\right)^{2\lambda+1} {}_1F_1\left(2\lambda+1; 2\lambda+2; -2\lambda\omega\left(2\pi - \frac{1}{2\omega} + \frac{2\pi e^{-4\pi\omega}}{\varrho_0}\right)\right)\right.\right.$$
$$\left.\left. - \left(\frac{2\pi e^{-4\pi\omega}}{\varrho_0} - \frac{1}{2\omega}\right)^{2\lambda+1} {}_1F_1\left(2\lambda+1; 2\lambda+2; -2\lambda\omega\left(\frac{2\pi e^{-4\pi\omega}}{\varrho_0} - \frac{1}{2\omega}\right)\right)\right\}\right]$$

4. Characterizations

In this section, we investigate several characterization properties of the proposed distribution. The results are established through two distinct approaches: (i) a relationship involving truncated moments and (ii) the hazard function. An important feature of the first characterization is that it does not require an explicit closed-form expression for the cumulative distribution function. Instead, the distribution can be identified through the solution of a first-order differential equation. This approach highlights the close connection between probabilistic models and differential-equation techniques, offering an alternative framework for characterizing the distribution.

4.1. Characterizations Based on Two Truncated Moments

This subsection develops characterization results for the proposed distribution by exploiting a relationship involving two truncated moments. The derivation is based on a theorem introduced by (Glänzel, 1987) (see Theorem 4.1). A noteworthy feature of this approach is its applicability beyond closed support intervals; the characterization remains valid even when the interval H is not closed. Furthermore, the method does not require an explicit analytical expression for the cumulative distribution function F, which enhances its usefulness in situations where the cdf is available only implicitly. As discussed by (Glänzel, 1990), the resulting characterization possesses a desirable stability property under weak convergence.

Theorem 4.1. *Let $(\Omega, \mathcal{F}, \mathbf{P})$ be a given probability space and let $H = [d, e]$ be an interval for some $d < e$ $(d = -\infty,\ e = \infty$ might as well be allowed$)$. Let $Y : \Omega \to H$ be a continuous random variable with the distribution function F and let q_1 and q_2 be two real functions defined on H such that*

$$\mathbf{E}\left[q_2(Y) \mid Y \geq y\right] = \mathbf{E}\left[q_1(Y) \mid Y \geq y\right]\eta(y), \quad y \in H,$$

is defined with some real function η. Assume that $q_1, q_2 \in C^1(H)$, $\eta \in C^2(H)$ and F is twice continuously differentiable and strictly monotone function on the set H. Finally, assume that the equation $\eta q_1 = q_2$ has no real solution in the interior of H. Then F is uniquely determined by the functions q_1, q_2 and η, particularly

$$F(y) = \int_a^y C\left|\frac{\eta'(u)}{\eta(u)q_1(u) - q_2(u)}\right|\exp(-s(u))\ du\ ,$$

where the function s is a solution of the differential equation $s' = \frac{\eta'\, q_1}{\eta\, q_1 - q_2}$ and C is the normalization constant, such that $\int_H dF = 1$.

Remark 1. The goal is to have $\eta(y)$ as simple as possible.

Proposition 4.2. *Let $Y : \Omega \to [0, 2\pi]$ be a continuous random variable and let $q_1(x) = [P(y)]^{-1}$ and $q_2(x) = q_1(x)e^{-2\omega y}$ for $y \in (0, 2\pi)$. The random variable X has pdf (1) if and only if the function η defined in Theorem 4.1 has the form*

$$\eta(x) = \frac{1}{2}\left[e^{-2\omega y} + e^{-4\omega\pi}\right], \quad y \in (0, 2\pi),$$

where $P(y) = \left(\omega^2y^2 - \omega y + 1\right)\rho_0^2 + \left(4\pi\omega^2 y - 2\pi\omega\right)e^{-4\pi\omega}\rho_0 + 4\pi^2\omega^2 e^{-4\pi\omega}\rho_1$.

Proof Let X be a random variable with pdf (1), then

$$(1-F(y))\,E\left[q_1(Y)\mid Y\geq y\right]=\int_y^{2\pi}\frac{2\omega}{\rho_0^3}e^{-2\omega u}du=\frac{1}{\rho_0^3}\left[e^{-2\omega y}-e^{-4\omega\pi}\right],\ \ y\in(0,2\pi),$$

and

$$(1-F(y))\,E\left[q_2(Y)\mid Y\geq y\right]=\int_y^{2\pi}\frac{2\omega}{\rho_0^3}e^{-4\omega u}du=\frac{1}{2\rho_0^3}\left[e^{-4\omega y}-e^{-8\omega\pi}\right],\ \ y\in(0,2\pi),$$

and finally

$$\eta(y)\,q_1(y)-q_2(y)=-\frac{q_1(y)}{2}\left[e^{-2\omega y}-e^{-4\omega\pi}\right]<0\quad for\ \ y\in(0,2\pi).$$

Conversely, if η is given as above, then

$$s'(x)=\frac{\eta'(y)\,q_1(y)}{\eta(y)\,q_1(y)-q_2(y)}=\frac{2\omega e^{-2\omega y}}{e^{-2\omega y}-e^{-4\omega\pi}},\quad y\in(0,2\pi),$$

and hence

$$s(y)=-\log\left\{e^{-2\omega y}-e^{-4\omega\pi}\right\},\quad\ y\in(0,2\pi).$$

Now, in view of Theorem 4.1, Y has density (1).

Corollary 4.3. *Let $X:\Omega\to[0,2\pi]$ be a continuous random variable and let $q_1(y)$ be as in Proposition 4.2. The pdf of Y is* (1) *if and only if there exist functions q_2 and η defined in Theorem 4.1 satisfying the differential equation*

$$\frac{\eta'(y)\,q_1(y)}{\eta(y)\,q_1(y)-q_2(y)}=\frac{2\omega e^{-2\omega y}}{e^{-2\omega y}-e^{-4\omega\pi}},\quad y\in(0,2\pi).$$

Corollary 4.4. *The general solution of the differential equation in Corollary 4.3 is*

$$\eta(y)=\left[e^{-2\omega y}-e^{-4\omega\pi}\right]^{-1}\left[-\int 2\omega e^{-2\omega y}\left(q_1(y)\right)^{-1}q_2(y)\,dy+D\right],$$

where D is a constant.

Proof. If Y has pdf (1), then clearly the differential equation holds. Now, if the differential equation holds, then

$$\eta'(y)=\left(\frac{2\omega e^{-2\omega y}}{e^{-2\omega y}-e^{-4\omega\pi}}\right)\eta(y)-\left(\frac{2\omega e^{-2\omega y}}{e^{-2\omega y}-e^{-4\omega\pi}}\right)\left(q_1(y)\right)^{-1}q_2(y),$$

or

$$\eta'(y)-\left(\frac{2\omega e^{-2\omega y}}{e^{-2\omega y}-e^{-4\omega\pi}}\right)\eta(y)=-\left(\frac{2\omega e^{-2\omega y}}{e^{-2\omega y}-e^{-4\omega\pi}}\right)\left(q_1(y)\right)^{-1}q_2(y),$$

or

$$\frac{d}{dy}\left\{\left[e^{-2\omega y}-e^{-4\omega\pi}\right]\eta(y)\right\}=-\left(2\omega e^{-2\omega y}\right)\left(q_1(y)\right)^{-1}q_2(y),$$

from which we arrive at

$$\eta(y)=\left[e^{-2\omega y}-e^{-4\omega\pi}\right]^{-1}\left[-\int 2\omega e^{-2\omega y}\left(q_1(y)\right)^{-1}q_2(y)\,dy+D\right].$$

Note that a set of functions satisfying the differential equation in Corollary 4.3, is given in Proposition 4.2 with $D=\frac{e^{-4\omega\pi}}{2}$. However, it should also be noted that there are other triplets (q_1,q_2,η) satisfying the conditions of Theorem 4.1.

4.2. Characterization in Terms of Hazard Function

The hazard function, h_F, of a twice differentiable distribution function, F, satisfies the following first order differential equation

$$\frac{f'(y)}{f(y)} = \frac{h'_F(y)}{h_F(y)} - h_F(y).$$

For most univariate continuous distributions, hazard function characterizations reduce to the standard differential equation form. The characterizations developed here go beyond this trivial form, offering genuinely distinct representations of the proposed distributions.

Proposition 4.5. *Let $Y : \Omega \to [0, 2\pi]$ be a continuous random variable. The random variable Y has pdf (1) if and only if its hazard function $h_F(y)$ satisfies the following differential equation*

$$h'_F(y) + 2\omega h_F(y)$$
$$= 2\omega e^{-2\omega y} \frac{d}{dy} \left\{ \frac{\left(\omega^2 y^2 - \omega y + 1\right) \varrho_0^2 + \left(4\pi\omega^2 y - 2\pi\omega\right) e^{-4\pi\omega} \varrho_0 + 4\pi^2\omega^2 e^{-4\pi\omega} \varrho_1}{\left[e^{-2\pi\omega}\left(1 + \omega^2 y^2\right) - e^{-4\pi\omega}\right] \varrho_0^2 + 4\omega^2\pi y e^{-2\omega(y+2\pi)} \varrho_0 - 4\omega^2\pi^2 e^{-4\pi\omega}(1 - e^{-2\omega y}) \varrho_1} \right\}, \quad y \in (0, 2\pi),$$

with the boundary condition $\lim_{x\to 0} h_F(x) = \frac{2\omega\left[\varrho_0 - 2\pi\omega e^{-4\pi\omega} \varrho_0 + 4\pi^2\omega^2 e^{-4\pi\omega} \varrho_1\right]}{\left[1 - e^{-4\pi\omega}\right]\varrho_0^2 - 4\pi^2\omega^2 e^{-4\pi\omega}(1 - e^{-2\omega y})\varrho_1}$.

5. Estimation of Model Parameters

5.1. Maximum Likelihood Estimation Method

For the purpose of parameter estimation, let $x_1, x_2, ..., x_n$ be a random sample of size n drawn from the WNPS distribution with parameter ω. The unknown parameter ω is estimated using the maximum likelihood estimation procedure, which is denoted by M_1 throughout this study. Accordingly, the likelihood function associated with the observed sample is given by

$$L(\omega) = \frac{(2\omega)^n e^{-2\omega \sum_{i=1}^n y_i}}{\varrho_0^{3n}} \prod_{i=1}^n \left[(\omega^2 y_i^2 - \omega y_i + 1)\varrho_0^2 + (4\pi\omega^2 y_i - 2\pi\omega) e^{-4\pi\omega} \varrho_0 + 4\pi^2\omega^2 e^{-4\pi\omega} \varrho_1\right]$$

Accordingly, the corresponding log-likelihood function takes the form

$$\ell(\omega) = n\ln(2\omega) - 2\omega \sum_{i=1}^n y_i - 2n\ln\varrho_0 + \sum_{i=1}^n \ln\left[(\omega^2 y_i^2 - \omega y_i + 1)\varrho_0^2 + (4\pi\omega^2 y_i - 2\pi\omega) e^{-4\pi\omega} \varrho_0 + 4\pi^2\omega^2 e^{-4\pi\omega} \varrho_1\right]$$

Taking the first derivative of the log-likelihood function with respect to ω, we obtain

$$\frac{d\ell(\omega)}{d\omega} = \frac{n}{\omega} - 2\sum_{i=1}^n y_i - \frac{12n\pi e^{-4\pi\omega}}{1 - e^{-4\pi\omega}} + \sum_{i=1}^n \frac{K_i(\omega)}{C_i(\omega)} \tag{13}$$

Where,

$$K_i(\omega) = (2\omega y_i^2 - y_i)\varrho_0^2 + 2\pi e^{-4\pi\omega} \varrho_0 (4\omega^2 y_i^2 + 4\omega y_i + 3)$$
$$+ 8\pi^2\omega e^{-4\pi\omega}\left[\left(2e^{-4\pi\omega} - 1\right)(2\omega y_i - 1) + \varrho_1\right] - 16\pi^3\omega^2 e^{-4\pi\omega}\left(1 + 2e^{-4\pi\omega}\right)$$

and

$$C_i(\omega) = (\omega^2 y_i^2 - \omega y_i + 1)\varrho_0^2 + (4\pi\omega^2 y_i - 2\pi\omega) e^{-4\pi\omega} \varrho_0 + 4\pi^2\omega^2 e^{-4\pi\omega} \varrho_1$$

The maximum likelihood estimate of ω is obtained by equating the first derivative of the log-likelihood function to zero and solving the resulting nonlinear equation using an appropriate numerical optimization technique.

5.2. Maximum Product of Spacings Estimation Method

In addition to the maximum likelihood approach, the parameters of the WNPS distribution can be estimated using the Maximum Product of Spacings (MPS) method, denoted by M_2. This method, originally proposed by (Cheng and Amin, 1983), is based on maximizing the geometric mean of the spacings between successive values of the fitted cumulative distribution function and has been shown to provide reliable estimates, particularly in situations where maximum likelihood estimation encounters numerical difficulties. The MPS estimator is obtained by maximizing the objective function given by

$$\Phi(y_i) = \frac{1}{n+1}\sum_{i=1}^{n+1} \log P_i(y_i),$$

Here, $P_i(y_{i:n}) = G(y_{i:n}) - G(y_{i-1:n}),\ \ G(y_{0:n}) = 0$ and $G(y_{n+1:n}) = 1$. Where, $G(y_i)$ denotes the cumulative distribution function of the WNPS distribution.

5.3. Least Square Estimation Method

Another method for estimating the parameter of the WNPS distribution is the Ordinary Least Squares Estimation (OLSE) method, denoted by M_3. Following the approach proposed by (Swain et al., 1988), the estimator is obtained by minimizing the squared differences between the theoretical cumulative distribution function and the expected values of the order statistics. The OLSE of ω is obtained by minimizing the objective function

$$\Theta_1(y_i) = \sum_{i=1}^{n}\left[G(y_{i:n}) - \frac{i}{n+1}\right]^2,$$

With respect to ω. where $G(y_i)$ denotes the cumulative distribution function of the WNPS distribution.
The Weighted Least Squares Estimation (WLSE) method, denoted by M_4, provides a weighted version of the OLSE procedure by incorporating the variances of the order statistics. According to Swain et al. (1988), the WLSE of ω is obtained by minimizing

$$\Theta_2(y_i) = \sum_{i=1}^{n}\frac{(n+1)^2(n+2)}{i(n-i+1)}\left[G(y_{i:n}) - \frac{i}{n+1}\right]^2,$$

with respect to ω.

5.4. Anderson-Darling Estimation Method

The Anderson–Darling Estimation (ADE) method, denoted by M_5, is another alternative for estimating the parameter of the WNPS distribution. This method is based on the Anderson–Darling goodness-of-fit criterion and assigns greater weight to observations in the tails of the distribution. Following (Anderson and Darling, 1952), the ADE of ω is obtained by minimizing the objective function

$$\eta(y_i) = -n - \frac{1}{n}\sum_{i=1}^{n}(2i-1)[\log G(y_{i:n}) + \log\{1 - G(y_{n-i+1:n})\}],$$

with respect to ω.

5.5. Cramér-von Mises Estimation Method

Following (Choi and Bulgren, 1968), the parameter ω is estimated using the Cramér-von Mises Estimation (CVME) method (M_6), which is based on minimizing the discrepancy between the theoretical and empirical distribution functions. The corresponding estimator is obtained by minimizing the following objective function

$$\Delta(y_i) = \frac{1}{12n} + \sum_{i=1}^{n}\left[G(y_{i:n}) - \frac{2i-1}{2n}\right]^2,$$

With respect to ω.

5.6. Percentiles Estimation Method

The Percentile Estimation Method (PCE), denoted by M_7, is also considered for estimating the parameter of the WNPS distribution. This approach is based on minimizing the squared differences between the observed order statistics and the corresponding theoretical quantiles of the distribution. Following (Kao, 1958), the estimate of ω is obtained by minimizing the following objective function with respect to ω:

$$\Xi(y_i) = \sum_{i=1}^{n} \left[x_{i:n} - Q\left(\frac{i}{n+1}\right)\right]^2,$$

Where, $Q(.)$ is the quantile function.

5.7. Minimum spacing absolute distance Estimation Method

Following the spacing-based estimation framework proposed by (Torabi, 2008), the parameter ω is estimated using the Minimum Spacing Absolute Distance (MSAD) method, denoted by M_8. The corresponding estimator is obtained by minimizing the following objective function with respect to ω:

$$\nu_1(y_i) = \sum_{i=1}^{n+1} \left| G_i - \frac{1}{n+1} \right|,$$

Where, $G_i = G(y_{i:n}) - G(y_{i-1:n})$.

5.8. Minimum spacing absolute-log distance Estimation Method

The Minimum Spacing Absolute Log-Distance (MSALD) method (M_9) is also employed for parameter estimation. Following (Torabi, 2008), the estimator of ω is obtained by minimizing an absolute log-distance measure based on the spacings of the fitted cumulative distribution function. Accordingly, the estimate of ω is determined by minimizing the following objective function:

$$\nu_2(y_i) = \sum_{i=1}^{n+1} \left| \log G_i - \log\left(\frac{1}{n+1}\right) \right|,$$

Where, $G_i = G(y_{i:n}) - G(y_{i-1:n})$.

5.9. Kolmogorov Estimation Method

Another estimation procedure employed in this study is the Kolmogorov Estimation Method (KM), denoted by M_{10}. Under this approach, the parameter ω is estimated by minimizing the Kolmogorov-Smirnov statistic, which measures the maximum deviation between the theoretical and empirical distribution functions (Aguilar et al., 2019). Thus, the corresponding estimator is given by

$$\zeta(y_i) = \max_{i \le i \le n} \left[\frac{i}{n} - G(y_i), G(y_i) - \frac{i-1}{n} \right]$$

5.10. Bayesian Estimation

Let $Y_1, Y_2, \ldots, Y_n$ be a random sample drawn from the WNPS distribution with parameter $\omega > 0$. The likelihood function based on the observed sample $\mathbf{y} = (y_1, y_2, \ldots, y_n)$ is given by

$$
\begin{aligned}
L(\omega \mid \mathbf{y}) &= \prod_{i=1}^{n} g(y_i;\omega) \\
&= \frac{(2\omega)^n \, e^{-2\omega \sum_{i=1}^{n} y_i}}{\varrho_0^{3n}} \prod_{i=1}^{n} \Big[(\omega^2 y_i^2 - \omega y_i + 1)\varrho_0^2 + (4\pi\omega^2 y_i - 2\pi\omega)\, e^{-4\pi\omega} \varrho_0 + 4\pi^2\omega^2 e^{-4\pi\omega} \varrho_1 \Big].
\end{aligned}
$$

Accordingly, the log-likelihood function takes the form

$$
\begin{aligned}
\ell(\omega) = n\log(2\omega) - 2\omega \sum_{i=1}^{n} y_i - 3n\log\varrho_0 + \sum_{i=1}^{n} \log\Big[(\omega^2 y_i^2 - \omega y_i + 1)\varrho_0^2 \\
+ (4\pi\omega^2 y_i - 2\pi\omega)\, e^{-4\pi\omega} \varrho_0 + 4\pi^2\omega^2 e^{-4\pi\omega} \varrho_1 \Big].
\end{aligned}
$$

To incorporate prior knowledge about ω, we assign a Gamma prior distribution with hyperparameters $a > 0$ and $b > 0$, having density

$$
\pi(\omega) = \frac{b^a}{\Gamma(a)}\, \omega^{a-1} e^{-b\omega}, \qquad \omega > 0. \tag{14}
$$

Applying Bayes' theorem, the posterior density of ω given the observed data is proportional to the product of the likelihood and the prior:

$$
\begin{aligned}
\pi(\omega \mid \mathbf{y}) \propto \frac{\omega^{n+a-1}\, e^{-\omega\left(b + 2\sum_{i=1}^{n} y_i\right)}}{\varrho_0^{3n}} \prod_{i=1}^{n} \Big[(\omega^2 y_i^2 - \omega y_i + 1)\varrho_0^2 \\
+ (4\pi\omega^2 y_i - 2\pi\omega)\, e^{-4\pi\omega} \varrho_0 + 4\pi^2\omega^2 e^{-4\pi\omega} \varrho_1 \Big].
\end{aligned}
$$

The normalized posterior density is therefore

$$
\begin{aligned}
\pi(\omega \mid \mathbf{y}) = \frac{1}{C} \frac{\omega^{n+a-1}\, e^{-\omega\left(b + 2\sum_{i=1}^{n} y_i\right)}}{\varrho_0^{3n}} \prod_{i=1}^{n} \Big[(\omega^2 y_i^2 - \omega y_i + 1)\varrho_0^2 \\
+ (4\pi\omega^2 y_i - 2\pi\omega)\, e^{-4\pi\omega} \varrho_0 + 4\pi^2\omega^2 e^{-4\pi\omega} \varrho_1 \Big]
\end{aligned}
$$

where the normalizing constant K is

$$
\begin{aligned}
C = \int_0^{\infty} \frac{\omega^{n+a-1}\, e^{-\omega\left(b + 2\sum_{i=1}^{n} y_i\right)}}{\varrho_0^{3n}} \prod_{i=1}^{n} \Big[(\omega^2 y_i^2 - \omega y_i + 1)\varrho_0^2 \\
+ (4\pi\omega^2 y_i - 2\pi\omega)\, e^{-4\pi\omega} \varrho_0 + 4\pi^2\omega^2 e^{-4\pi\omega} \varrho_1 \Big]\, d\omega.
\end{aligned} \tag{15}
$$

Since the posterior density of ω does not correspond to any standard distributional family, a closed-form expression for the Bayes estimator is not attainable. Accordingly, numerical methods are employed: the Metropolis-Hastings (MH) algorithm is used to generate posterior samples.

In this study, we employ a variety of symmetric and asymmetric loss functions(LF), including the SELF, WSELF, MSELF, KLF and LINEX loss functions. The corresponding Bayesian estimators (BS) and posterior risks (PR) associated with these loss functions are summarized in Table 2. For more details about the loss functions, see (Ahmad et al., 2020).

Table 2: Bayes estimators and posterior risks under different loss functions for the parameter ω of the WNPS distribution

Loss Function	Bayes Estimator	Posterior Risk
SELF : $L(\omega, d) = (\omega - d)^2$	$E(\omega\|\mathbf{y})$	$Var(\omega\|\mathbf{y})$
WSELF : $L(\omega, d) = \dfrac{(\omega - d)^2}{\omega}$	$\big(E(\omega^{-1}\|\mathbf{y})\big)^{-1}$	$E(\omega\|\mathbf{y}) - \big(E(\omega^{-1}\|\mathbf{y})\big)^{-1}$
MSELF : $L(\omega, d) = \left(1 - \dfrac{d}{\omega}\right)^2$	$\dfrac{E(\omega^{-1}\|\mathbf{y})}{E(\omega^{-2}\|\mathbf{y})}$	$1 - \dfrac{\big(E(\omega^{-1}\|\mathbf{y})\big)^2}{E(\omega^{-2}\|\mathbf{y})}$
KLF : $L(\omega, d) = \left(\sqrt{\dfrac{d}{\omega}} - \sqrt{\dfrac{\omega}{d}}\right)^2$	$\sqrt{\dfrac{E(\omega\|\mathbf{y})}{E(\omega^{-1}\|\mathbf{y})}}$	$2\left(\sqrt{E(\omega\|\mathbf{y})E(\omega^{-1}\|\mathbf{y})} - 1\right)$
LINEX : $L(\omega, d) = e^{\,c(d-\omega)} - c(d - \omega) - 1$	$-\dfrac{1}{c}\log\big(E\big(e^{-c\omega} \mid \mathbf{y}\big)\big)$	$c\,E(\omega\|\mathbf{y}) + \log E\big(e^{-c\omega} \mid \mathbf{y}\big)$

5.10.1. MCMC Procedure Using the Metropolis-Hastings Algorithm

The posterior distribution of ω under the WQL model does not belong to any recognizable standard family, precluding closed-form Bayes estimators. To circumvent this, Markov Chain Monte Carlo (MCMC) sampling is adopted. Specifically, the Metropolis–Hastings (MH) algorithm is applied to draw samples from $\pi(\omega \mid \mathbf{y})$, from which posterior-based estimates of ω are subsequently derived. The complete sampling procedure is detailed in Algorithm 1.

5.11. Credible Interval

A posterior credible interval quantifies parameter uncertainty directly from the posterior distribution. Let $\omega^{(M+1)}, \omega^{(M+2)}, \ldots, \omega^{(N)}$ denote the post-burn-in samples retained from the MH algorithm.

5.11.1. Equal-Tail Credible Interval

The $100(1-\alpha)\%$ equal-tail credible interval (ETCI) is constructed by trimming equal probability mass from both tails of the posterior. The 95% credible interval is given by

$$\mathrm{CI}_{95\%} = \left[Q_{0.025}(\omega \mid \mathbf{y}),\ Q_{0.975}(\omega \mid \mathbf{y})\right], \tag{16}$$

where $Q_p(\omega \mid \mathbf{y})$ denotes the pth posterior quantile. The bounds are estimated empirically as

$$\begin{aligned}\widehat{\omega}_L &= \mathrm{Quantile}\Big(\{\omega^{(t)}\}_{t=M+1}^{N},\ 0.025\Big),\\ \widehat{\omega}_U &= \mathrm{Quantile}\Big(\{\omega^{(t)}\}_{t=M+1}^{N},\ 0.975\Big).\end{aligned} \tag{17}$$

5.11.2. Highest Posterior Density Interval

The highest posterior density (HPD) interval is the shortest interval containing a specified posterior probability, ensuring every interior point has higher posterior density than any exterior point. The $100(1-\alpha)\%$ HPD interval is defined as

$$\mathrm{HPD}_{1-\alpha} = \{\omega : \pi(\omega \mid \mathbf{y}) \geq k_\alpha\}, \tag{18}$$

where k_α is the largest constant satisfying $P(\omega \in \mathrm{HPD}_{1-\alpha} \mid \mathbf{y}) \geq 1 - \alpha$. Using the ordered post-burn-in samples $\omega^{(1)} \leq \omega^{(2)} \leq \cdots \leq \omega^{(N-M)}$, the HPD bounds are obtained as

$$(\widehat{\omega}_L^*,\ \widehat{\omega}_U^*) = \arg\min_j \left\{\omega^{(j+\lfloor(1-\alpha)(N-M)\rfloor)} - \omega^{(j)}\right\}, \quad j = 1, \ldots, \lfloor\alpha(N-M)\rfloor. \tag{19}$$

Unlike the ETCI, the HPD interval is not necessarily symmetric about the posterior mean, making it more informative for skewed posteriors.

 DOI: http://dx.doi.org/10.18187/pjsor.v22i3.4923

Algorithm 1 Metropolis–Hastings Algorithm for Bayesian Estimation of the WNPS Model

Set an initial value $\omega^{(0)} > 0$.
Fix the number of MCMC iterations N, the burn-in size M, and the proposal variance σ^2.
for $t = 1, 2, \ldots, N$ **do**
  Generate a candidate value from the random-walk proposal distribution:

$$\omega^* \sim N\left(\omega^{(t-1)}, \sigma^2\right).$$

  if $\omega^* \leq 0$ **then**
    Set $\omega^{(t)} = \omega^{(t-1)}$.
  else
    Evaluate the posterior density at the proposed and current values.
    Compute

$$A = \frac{\pi(\omega^*|\mathbf{y})q(\omega^{(t-1)}|\omega^*)}{\pi(\omega^{(t-1)}|\mathbf{y})q(\omega^*|\omega^{(t-1)})}.$$

    Define the acceptance probability as $\alpha = \min\{1, A\}$.
    Generate a random number $u \sim U(0, 1)$.
    if $u \leq \alpha$ **then**
      Accept the proposed value: $\omega^{(t)} = \omega^*$.
    else
      Retain the current value: $\omega^{(t)} = \omega^{(t-1)}$.
    end if
  end if
end for
Remove the first M simulated values as burn-in.
The posterior sample is given by $\left\{\omega^{(M+1)}, \omega^{(M+2)}, \ldots, \omega^{(N)}\right\}$.
Compute the Bayes estimates of ω under SELF, WSELF, MSELF, KLF, and LINEX loss functions from the retained posterior samples.

6. Finite-Sample Performance Analysis

A Monte Carlo simulation study is conducted to assess the performance of the ten estimation methods considered in this work. For each parameter setting, $l = 10,000$ replications are generated across five different sample sizes (n=30, 75, 150, 250, and 400). The performance of the estimators is evaluated using Bias, Mean Squared Error (MSE), and Mean Relative Error (MRE). The expressions for Bias, MSE, and MRE are respectively given by:

$$\text{Bias} = \frac{1}{l}\sum_{i=1}^{l}(\hat{\omega}_i - \omega), \;\; \text{MSE} = \frac{1}{l}\sum_{i=1}^{l}(\hat{\omega}_i - \omega)^2, \;\; \text{MRE} = \frac{1}{l}\sum_{i=1}^{l}\left|\frac{\hat{\omega}_i - \omega}{\omega}\right|$$

The numerical results obtained from the simulation study are presented in Tables 3–5, while the corresponding heatmap diagrams are displayed in Figures 3–5. Based on these results, the principal findings of the simulation analysis may be summarized as follows:

1. Overall, the Bias, MSE, and MRE exhibit a decreasing trend with increasing sample size, indicating improved estimator performance.

2. Among the estimation methods examined, M_5 (AD) generally yields the smallest bias across the majority of sample sizes. In contrast, M_2 (MPS) demonstrates superior overall performance in terms of MSE and MRE, attaining the lowest values for these measures in most simulation settings. On the other hand, M_7 (PCE) tends to exhibit relatively larger bias values, whereas M_{10} (KM) produces the highest MSE and MRE values across nearly all sample sizes, indicating comparatively weaker estimation performance.

3. The overall findings indicate that M_2 (MPS) and M_5 (AD) provide the most reliable estimates, whereas M_6 (CVM) and M_{10} (KM) tend to be less efficient across the simulation scenarios examined.

4. Figures 3-5 provide a visual summary of the simulation results through heatmaps, highlighting a systematic decrease in Bias, MSE, and MRE as the sample size increases across all considered parameter values. The gradual reduction in colour intensity for larger samples indicates improved estimation accuracy and confirms the asymptotic efficiency of the estimators.

Pak.j.stat.oper.res. Vol.22 No.3 2026 pp 433-458

Table 3: Performance of the WNPS distribution based on simulation experiments $(\omega = 0.8)$

n	Measure	M_1	M_2	M_3	M_4	M_5	M_6	M_7	M_8	M_9	M_{10}
30	Mean	0.835379	0.776520	0.825178	0.823256	0.818315	0.830568	0.773896	0.826903	0.780433	0.833329
	Bias	0.035379	-0.023480	0.025178	0.023256	0.018315	0.030568	-0.026104	0.026903	-0.019567	0.033329
	MSE	0.033438	0.027634	0.051044	0.044671	0.039542	0.051706	0.030012	0.086602	0.035803	0.052222
	MRE	0.172368	0.162673	0.213544	0.199262	0.191406	0.214453	0.169830	0.237864	0.183023	0.216877
75	Mean	0.813952	0.785808	0.810540	0.810070	0.807733	0.812791	0.783262	0.798629	0.788637	0.813372
	Bias	0.013952	-0.014193	0.010540	0.010070	0.007733	0.012791	-0.016738	-0.001371	-0.011363	0.013372
	MSE	0.011214	0.010214	0.018291	0.015372	0.014623	0.018407	0.011070	0.018279	0.013440	0.018804
	MRE	0.103549	0.100733	0.132793	0.121394	0.119283	0.133027	0.104827	0.130645	0.114738	0.134678
150	Mean	0.806521	0.790975	0.805030	0.804978	0.803735	0.806169	0.789321	0.797549	0.792484	0.806656
	Bias	0.006521	-0.009025	0.005030	0.004978	0.003735	0.006169	-0.010679	-0.002451	-0.007516	0.006656
	MSE	0.005445	0.005171	0.008858	0.007365	0.007203	0.008887	0.005586	0.009007	0.006877	0.009180
	MRE	0.072874	0.071936	0.092830	0.084461	0.083723	0.092918	0.074922	0.093732	0.082501	0.094420
250	Mean	0.803626	0.793771	0.801659	0.802020	0.801159	0.802344	0.792871	0.797637	0.794889	0.802537
	Bias	0.003626	-0.006229	0.001659	0.002020	0.001159	0.002344	-0.007129	-0.002363	-0.005111	0.002537
	MSE	0.003191	0.003089	0.005264	0.004355	0.004304	0.005273	0.003261	0.005052	0.004234	0.005391
	MRE	0.055991	0.055493	0.072075	0.065432	0.065179	0.072103	0.056972	0.070527	0.064890	0.073229
400	Mean	0.801784	0.795386	0.801043	0.801230	0.800594	0.801472	0.794895	0.797184	0.795990	0.801561
	Bias	0.001784	-0.004614	0.001043	0.001230	0.000594	0.001472	-0.005105	-0.002816	-0.004010	0.001561
	MSE	0.001915	0.001880	0.003255	0.002665	0.002637	0.003258	0.002003	0.003072	0.002571	0.003293
	MRE	0.043551	0.043365	0.056731	0.051248	0.051045	0.056739	0.044757	0.054790	0.050479	0.057176

DOI: http://dx.doi.org/10.18187/pjsor.v22i3.4923

Pak.j.stat.oper.res. Vol.22 No.3 2026 pp 433-458

DOI: http://dx.doi.org/10.18187/pjsor.v22i3.4923

Table 4: Performance of the WNPS distribution based on simulation experiments $(\omega = 2.5)$

n	Measure	M_1	M_2	M_3	M_4	M_5	M_6	M_7	M_8	M_9	M_{10}
30	Mean	2.623732	2.429591	2.585503	2.579536	2.564163	2.603060	2.425937	2.565640	2.443666	2.609321
	Bias	0.123732	-0.070409	0.085503	0.079536	0.064163	0.103060	-0.074063	0.065640	-0.056334	0.109321
	MSE	0.302710	0.251657	0.470600	0.409307	0.359856	0.476274	0.272304	0.586259	0.321652	0.482124
	MRE	0.163905	0.157532	0.207311	0.192833	0.184605	0.207932	0.163857	0.213693	0.176447	0.210707
75	Mean	2.548560	2.450836	2.539722	2.537784	2.529894	2.546972	2.443800	2.498040	2.459839	2.546947
	Bias	0.048560	-0.049164	0.039722	0.037784	0.029894	0.046972	-0.056200	-0.001960	-0.040161	0.046947
	MSE	0.099844	0.092860	0.172609	0.144006	0.135343	0.173704	0.100155	0.166661	0.121315	0.177532
	MRE	0.098994	0.097502	0.128876	0.117505	0.115152	0.129092	0.101361	0.125966	0.111021	0.131168
150	Mean	2.524543	2.468002	2.518125	2.518247	2.513843	2.521788	2.461167	2.490772	2.473385	2.522366
	Bias	0.024543	-0.031998	0.018125	0.018247	0.013843	0.021788	-0.038833	-0.009228	-0.026615	0.022366
	MSE	0.048204	0.046635	0.082525	0.067640	0.065730	0.082783	0.050978	0.078976	0.062679	0.084008
	MRE	0.068975	0.069086	0.090341	0.081604	0.080726	0.090410	0.072490	0.088787	0.079578	0.091339
250	Mean	2.513002	2.475579	2.507636	2.508350	2.505474	2.509829	2.470666	2.489985	2.479732	2.509707
	Bias	0.013002	-0.024421	0.007636	0.008350	0.005474	0.009829	-0.029334	-0.010015	-0.020268	0.009707
	MSE	0.028058	0.027665	0.048414	0.039503	0.039000	0.048495	0.030101	0.044176	0.037472	0.049590
	MRE	0.053154	0.053339	0.069877	0.063084	0.062835	0.069897	0.055505	0.066724	0.061753	0.070764
400	Mean	2.506961	2.481642	2.502478	2.503656	2.501566	2.503852	2.477729	2.489868	2.482369	2.504144
	Bias	0.006961	-0.018358	0.002478	0.003656	0.001566	0.003852	-0.022271	-0.010132	-0.017631	0.004144
	MSE	0.017393	0.017350	0.030831	0.025050	0.024847	0.030857	0.018670	0.028361	0.023340	0.031526
	MRE	0.041967	0.042230	0.055630	0.050086	0.049983	0.055640	0.043946	0.053773	0.048774	0.056485

Pak.j.stat.oper.res. Vol.22 No.3 2026 pp 433-458

Table 5: Performance of the WNPS distribution based on simulation experiments $(\omega = 3.5)$

n	Measure	M_1	M_2	M_3	M_4	M_5	M_6	M_7	M_8	M_9	M_{10}
30	Mean	3.675129	3.402943	3.623537	3.615442	3.593252	3.648166	3.397878	3.571003	3.421866	3.657446
	Bias	0.175129	-0.097057	0.123537	0.115442	0.093252	0.148166	-0.102122	0.071003	-0.078134	0.157446
	MSE	0.589828	0.488858	0.926927	0.809157	0.709683	0.938508	0.528139	1.036340	0.620757	0.955774
	MRE	0.163787	0.157043	0.207440	0.192991	0.184641	0.208098	0.163029	0.211116	0.175579	0.211338
75	Mean	3.568767	3.432203	3.551526	3.549615	3.538809	3.561681	3.422920	3.499844	3.442135	3.563256
	Bias	0.068767	-0.067797	0.051526	0.049615	0.038809	0.061681	-0.077080	-0.000156	-0.057865	0.063256
	MSE	0.197412	0.183296	0.334161	0.278807	0.263645	0.336208	0.198759	0.323890	0.239953	0.345057
	MRE	0.098936	0.097975	0.129532	0.117911	0.115625	0.129707	0.101923	0.125863	0.111285	0.131658
150	Mean	3.532675	3.453497	3.524711	3.524617	3.518799	3.529831	3.444685	3.489072	3.459189	3.531498
	Bias	0.032675	-0.046503	0.024711	0.024617	0.018799	0.029831	-0.055315	-0.010928	-0.040811	0.031498
	MSE	0.095599	0.092627	0.162060	0.133574	0.130229	0.162574	0.100964	0.162227	0.122523	0.168540
	MRE	0.069664	0.069886	0.090678	0.082101	0.081301	0.090747	0.073157	0.090902	0.079862	0.092405
250	Mean	3.518205	3.465797	3.509079	3.510798	3.506752	3.512155	3.458491	3.487196	3.470368	3.512727
	Bias	0.018205	-0.034203	0.009079	0.010798	0.006752	0.012155	-0.041509	-0.012804	-0.029632	0.012727
	MSE	0.055933	0.055179	0.096252	0.078835	0.077764	0.096408	0.059173	0.090919	0.075257	0.098868
	MRE	0.053493	0.053771	0.070421	0.063588	0.063306	0.070439	0.055725	0.068512	0.062621	0.071672
400	Mean	3.509476	3.474025	3.505687	3.506615	3.503627	3.507611	3.468031	3.484331	3.475931	3.507795
	Bias	0.009476	-0.025975	0.005687	0.006615	0.003627	0.007611	-0.031969	-0.015669	-0.024069	0.007795
	MSE	0.033561	0.033502	0.059575	0.048264	0.047688	0.059633	0.036207	0.055108	0.045649	0.060448
	MRE	0.041645	0.041939	0.055460	0.049817	0.049603	0.055463	0.043607	0.053119	0.048718	0.055990

DOI: http://dx.doi.org/10.18187/pjsor.v22i3.4923

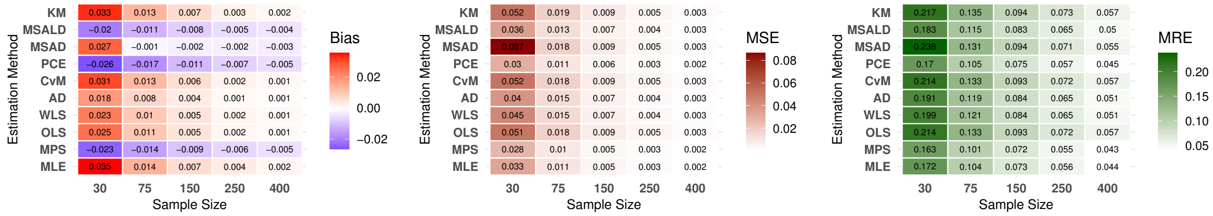

Figure 3: Simulation-based heatmaps of Bias, MSE, and MRE corresponding to $\omega = 0.8$

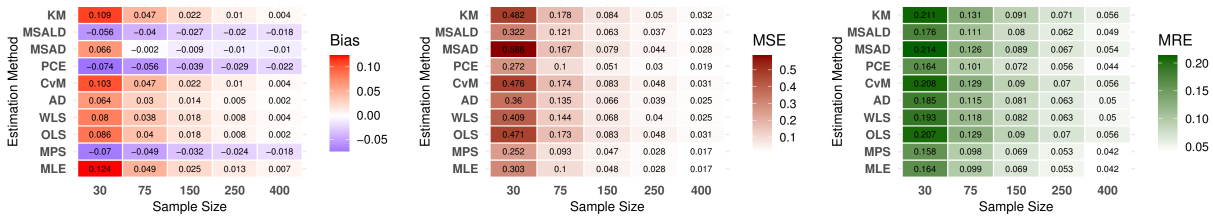

Figure 4: Simulation-based heatmaps of Bias, MSE, and MRE corresponding to $\omega = 2.5$

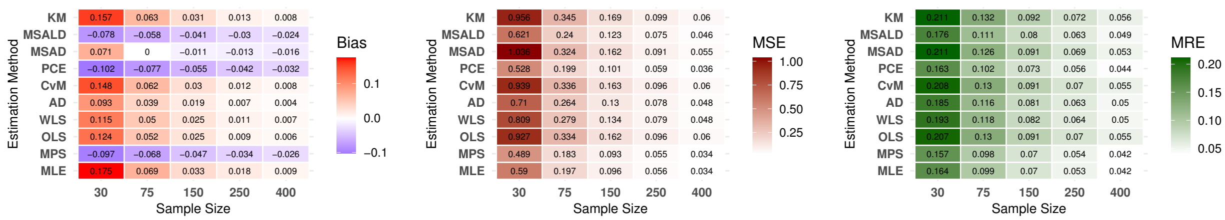

Figure 5: Simulation-based heatmaps of Bias, MSE, and MRE corresponding to $\omega = 3.5$

6.1. Simualtion Study under Bayesian Estimation

To assess the sample performance of the proposed Bayesian estimators, a Monte Carlo simulation study is conducted. Samples of sizes n=40, 75, 150, and 250 are drawn from the WNPS distribution at true parameter values $\omega = 0.45, 1.8,$ and 3.0. Estimation is carried out under a Gamma prior $\omega \sim \text{Gamma}(a, b)$ with hyperparameters (a,b)=(1,2) , and five loss functions as listed in Table 2 are employed throughout. For each simulation configuration, the MH algorithm is run for 10,000 iterations, discarding the first 1,000 as burn-in. The PR is evaluated under each estimator's own loss function. Table 6 reveals that posterior risk decreases consistently as n increases, confirming estimator consistency. Among all loss functions, the LINEX-based estimator achieves the lowest posterior risk across all parameter values and sample sizes. The MSELF and KLF estimators perform nearly identically throughout. Additionally, posterior risk increases with ω for fixed n, reflecting greater uncertainty at larger parameter scales. Overall, the LINEX loss is recommended for Bayesian estimation of the WNPS model parameter.

7. Applied Relevance of the Model

This section elucidates the superiority of the proposed model relative to seven existing competing models. The considered models include Wrapped Lindley (WL) (Joshi and Jose, 2018), Wrapped XLindley (WXL) (Zinhom et al., 2023), Wrapped Modified Lindley (WML) (Chesneau et al., 2021), Wrapped Shanker (WS) (Al-Meanazel and Al-Khazaleh, 2021), Wrapped Two-Parameter Lindley (WTPL) (Bhattacharjee et al., 2021), and Von-Mises (VM) (Mardia and Jupp, 2009). The unknown parameters of all models are estimated using the maximum likelihood estimation method. To validate the goodness-of-fit in real-world applications, several model selection criteria, namely Akaike Information Criterion (C_1), Akaike Information Criterion Corrected (C_2), Bayesian Information Criterion (C_3), Hannan–Quinn Information Criterion (C_4), and Consistent Akaike Information Criterion (C_5), together with the Kolmogorov–Smirnov statistic (K-Statistic), are employed.

Table 6: Simulation-Based Posterior Risk of Bayesian Estimators Under Various Loss Functions for the WNPS Distribution

$n = 40$	$\omega = 0.45$	$\omega = 1.8$	$\omega = 3.0$
Loss function	$r_{\hat{\omega}}$	$r_{\hat{\omega}}$	$r_{\hat{\omega}}$
SELF	0.010968	0.080290	0.264844
WSELF	0.026352	0.048703	0.104320
MSELF	0.071710	0.030906	0.041597
KLF	0.067731	0.030720	0.042123
LINEX	0.001363	0.009832	0.032462
$n = 75$	$\omega = 0.45$	$\omega = 1.8$	$\omega = 3.0$
Loss function	$r_{\hat{\omega}}$	$r_{\hat{\omega}}$	$r_{\hat{\omega}}$
SELF	0.006106	0.041040	0.125796
WSELF	0.014704	0.023864	0.046564
MSELF	0.037470	0.014287	0.017495
KLF	0.036005	0.014086	0.017271
LINEX	0.000762	0.005081	0.015608
$n = 150$	$\omega = 0.45$	$\omega = 1.8$	$\omega = 3.0$
Loss function	$r_{\hat{\omega}}$	$r_{\hat{\omega}}$	$r_{\hat{\omega}}$
SELF	0.003308	0.022021	0.063864
WSELF	0.007681	0.012498	0.022490
MSELF	0.018390	0.007198	0.008004
KLF	0.017935	0.007052	0.007851
LINEX	0.000413	0.002754	0.008000
$n = 250$	$\omega = 0.45$	$\omega = 1.8$	$\omega = 3.0$
Loss function	$r_{\hat{\omega}}$	$r_{\hat{\omega}}$	$r_{\hat{\omega}}$
SELF	0.001961	0.013870	0.039519
WSELF	0.004491	0.007790	0.013580
MSELF	0.010485	0.004413	0.004701
KLF	0.010346	0.004384	0.004673
LINEX	0.000245	0.001732	0.004932

7.1. First Dataset

The first dataset, presented by (Fisher, 1995), represents the orientation measurements of 50 Starhead Topminnows recorded under cloudy sky conditions.
Table 7 depicts the better performance of the WNPS model over the WL, WXL, WML, WS, WTPL, and VM models for the first dataset based on all the considered model selection criteria. The K-statistic also supports the superiority of the WNPS model. Furthermore, the negative log-likelihood values, estimated parameter values, and their corresponding standard errors are provided.
Figure 6 presents the rose diagram and fitted density curves for the first dataset. The fitted density plots indicate that the WNPS model provides a closer fit to the observed histogram than the competing models. Furthermore, Figure 7 shows the estimated CDF and survival function plots, which also support the superior performance of the WNPS model for the first dataset.

7.2. Second Dataset

The second dataset considered in this study is the speed.wind2 dataset from the NPCirc package in R. It consists of 200 hourly observations of wind direction and wind speed recorded by an oceanographic buoy off the Atlantic coast of Galicia, Spain. For the present analysis, a random sample of 100 observations was selected from the dataset. The data are a lagged subset of winter-season observations collected during 2003–2012((Oliveira et al., 2014)).
As shown in Table 8, the WNPS model exhibits the best overall performance among the WL, WXL, WML, WS, WTPL, and VM models for the second dataset according to all the considered model selection measures. The K-statistic also favors the WNPS model. Moreover, the corresponding negative log-likelihood values, estimated parameters, and standard errors are presented.

Table 7: Parameter estimation and model selection criteria for the first dataset

Model	$-l$	C_1	C_2	C_3	C_4	C_5	K-Statistic	Estimated parameters (S.E.)
WNPS	90.7646	183.5291	183.6124	185.4411	184.2572	186.4411	0.0531	$\hat{\omega} = 0.0614(0.0425)$
WL	91.2607	184.5215	184.6048	186.4335	185.2496	187.4335	0.4843	$\hat{\lambda} = 0.3149(0.1397)$
WXL	91.0189	184.0378	184.1211	185.9498	184.7659	186.9498	0.0686	$\hat{\lambda} = 0.2644(0.1120)$
WML	91.6769	185.3539	185.4372	187.2659	186.0820	188.2659	0.1021	$\hat{\lambda} = 0.2078(0.1189)$
WS	91.7010	185.4020	185.4854	187.3141	186.1301	188.3141	0.0971	$\hat{\lambda} = 0.3727(0.1542)$
WTPL	91.8939	187.7877	188.0430	191.6118	189.2439	193.6118	0.1283	$\hat{\lambda} = 1 \times e^{-4}(0.0124)$
								$\hat{\alpha} = 9.4991(11284.36)$
VM	90.2635	184.5270	184.7824	188.3511	185.9833	190.3511	0.0645	$\hat{\omega} = 1.0607(0.5515)$
								$\hat{\kappa} = 0.3656(0.2050)$

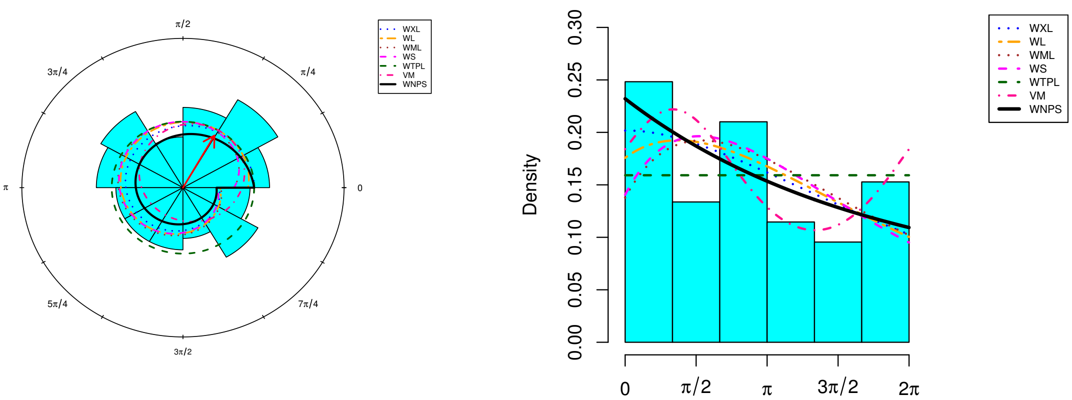

Figure 6: Rose diagram and Histogram illustrating the first dataset

The rose diagram and fitted density functions for the first dataset are presented in Figure 8. Among the fitted models, the WNPS distribution exhibits the closest agreement with the empirical histogram. This finding is further reinforced by the estimated cdf and survival function plots shown in Figure 9, which indicate the superior performance of the WNPS model.

Table 8: Parameter estimation and model selection criteria for the second dataset

Model	$-l$	C_1	C_2	C_3	C_4	C_5	K-Statistic	Estimated parameters (S.E.)
WNPS	180.6725	363.3450	363.3858	365.9502	364.3993	366.9502	0.1066	$\hat{\omega} = 0.0721(0.0305)$
WL	181.7188	365.4376	365.4784	368.0427	366.4919	369.0427	0.4008	$\hat{\lambda} = 0.3547(0.0900)$
WXL	181.1737	364.3474	364.3882	366.9526	365.4018	367.9526	0.1246	$\hat{\lambda} = 0.2953(0.0744)$
WML	182.7005	367.4010	367.4418	370.0061	368.4553	371.0061	0.1606	$\hat{\lambda} = 0.2444(0.0707)$
WS	182.6207	367.2414	367.2822	369.8466	368.2958	370.8466	0.1534	$\hat{\lambda} = 0.4205(0.0898)$
WTPL	183.7877	371.5754	371.6991	376.7858	373.6841	378.7858	0.1944	$\hat{\lambda} = 0.1364(0.1062)$
								$\hat{\alpha} = 1 \times e^{-4}(0.0903)$
VM	182.0715	368.1430	368.2667	373.3533	370.2517	375.3533	0.1355	$\hat{\omega} = 0.7614(0.5386)$
								$\hat{\kappa} = 0.2637(0.1433)$

The parameter estimates and associated model selection criteria for the WNPS distribution, obtained under various estimation methods for the two datasets, are presented in Table 9.

The results of our Bayesian analysis, both numerical and graphical, are provided for the two data sets under study.

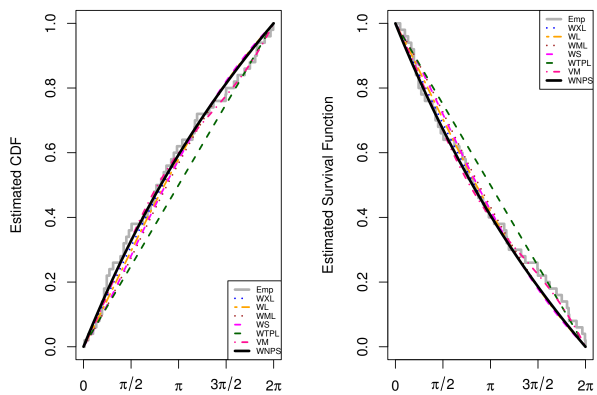

Figure 7: Est. cdf and Survival function for the first dataset

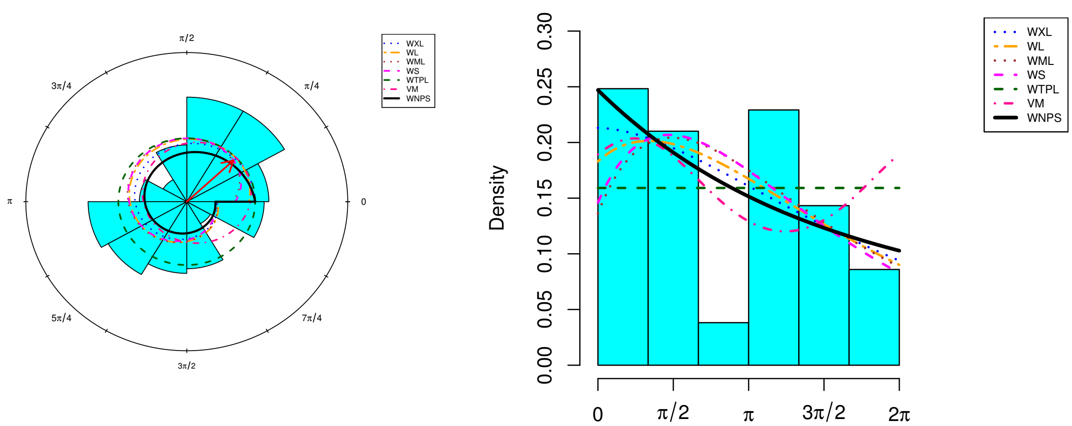

Figure 8: Rose diagram and Histogram illustrating the second dataset

The Bayesian estimates of the WNPS distribution parameter are derived from the loss functions presented in Table 2. The Bayesian analysis is performed based on the Metropolis-Hastings MCMC method that involves 10,000 iterations and a burn-in of 1,000 iterations. Table 10 reflects the Bayesian point estimates together with their respective posterior risks of the parameter ω of the suggested WNPS model based on different types of loss functions. It is noted that posterior risks obtained using the LINEX and SELF loss functions are found to be lower than those derived using other loss functions. Besides, the 95% credible intervals and Highest Posterior Density(HPD) intervals can serve as good measures of the degree of uncertainty surrounding the Bayesian estimates. Figures 10 and 11 present the MCMC diagnostic plots for two datasets. The trace plots indicate good mixing and convergence of the Markov chains, while the posterior density plots suggest unimodal posterior distributions for the parameter ω. In addition, the autocorrelation functions decrease rapidly with increasing lag, indicating relatively low dependence among successive posterior samples. These results confirm the adequacy of the Metropolis-Hastings algorithm for Bayesian estimation of the proposed model.

8. Conclusions

This study introduced the Wrapped New Polynomial Single-Parameter (WNPS) distribution, a parsimonious one-parameter circular model obtained by wrapping the New Polynomial Single-Parameter distribution onto the unit cir-

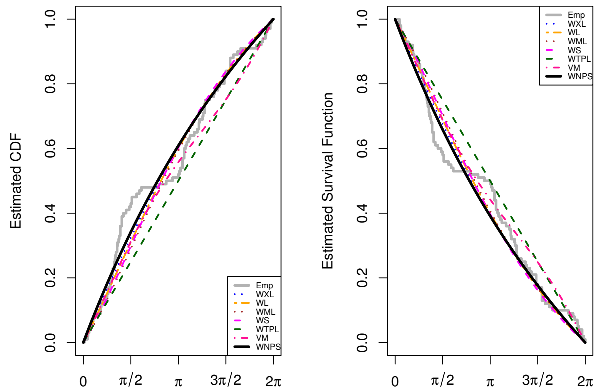

Figure 9: Est. cdf and Survival function for the second dataset

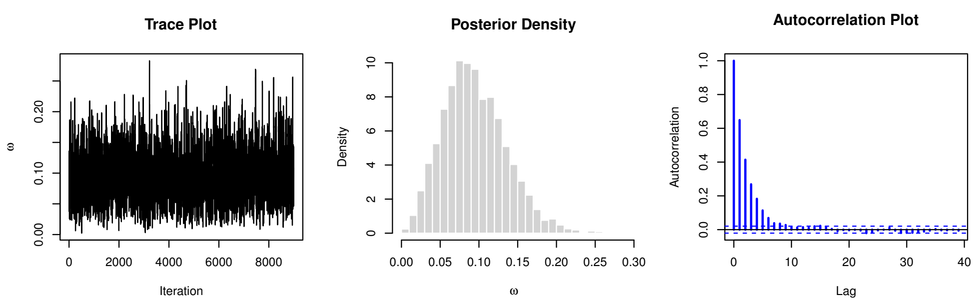

Figure 10: Trace plot, posterior density plot, and autocorrelation function of the MCMC samples for the parameter ω of the WNPS model for first Dataset.

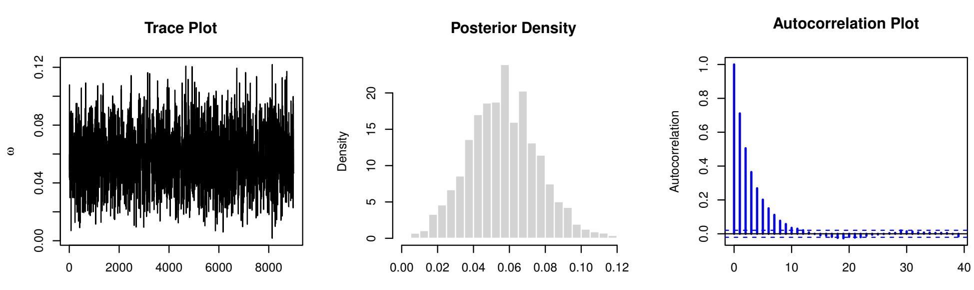

Figure 11: Trace plot, posterior density plot, and autocorrelation function of the MCMC samples for the parameter ω of the WNPS model for second Dataset.

Table 9: Estimated model parameters and associated information criteria for the WNPS model across all datasets

	First Dataset								
Stat.	M_2	M_3	M_4	M_5	M_6	M_7	M_8	M_9	M_{10}
$\widehat{\omega}$	0.0330	0.0661	0.0628	0.0609	0.0659	0.0601	0.0723	0.0491	0.0621
K-Statistic	0.0864	0.0488	0.0518	0.0534	0.0490	0.0542	0.0431	0.0655	0.0524
C_1	183.9977	183.5415	183.5302	183.5292	183.5402	183.5300	183.5943	183.6140	183.5294
C_2	184.0811	183.6249	183.6135	183.6125	183.6236	183.6134	183.6777	183.6974	183.6127
C_3	185.9098	185.4535	185.4422	185.4412	185.4523	185.4420	185.5064	185.5261	185.4414
C_4	184.7258	184.2696	184.2583	184.2573	184.2683	184.2581	184.3224	184.3421	184.2575
C_5	186.9098	186.4535	186.4422	186.4412	186.4523	186.4420	186.5064	186.5261	186.4414
	Second Dataset								
Stat.	M_2	M_3	M_4	M_5	M_6	M_7	M_8	M_9	M_{10}
$\widehat{\omega}$	0.0736	0.0736	0.0714	0.0719	0.0735	0.0688	0.0976	0.0911	0.0752
K-Statistic	0.1048	0.1048	0.1074	0.1068	0.1049	0.1105	0.1223	0.1141	0.1029
C_1	363.3475	363.3474	363.3456	363.3450	363.3472	363.3571	364.0010	363.7165	363.3552
C_2	363.3884	363.3882	363.3864	363.3858	363.3880	363.3979	364.0418	363.7573	363.3960
C_3	365.9527	365.9526	365.9507	365.9502	365.9523	365.9622	366.6062	366.3217	365.9604
C_4	364.4019	364.4018	364.3999	364.3994	364.4015	364.4114	365.0554	364.7709	364.4096
C_5	366.9527	366.9526	366.9507	366.9502	366.9523	366.9622	367.6062	367.3217	366.9604

Table 10: Bayesian estimates, posterior risks, and 95% credible and HPD intervals for the WNPS distribution.

	Dataset 1		Dataset 2	
LF	Estimate	PR	Estimate	PR
SELF	0.094763	0.001671	0.056715	0.000371
WSELF	0.072197	0.022566	0.047679	0.009036
MSELF	0.035636	0.506412	0.027780	0.417360
KLF	0.082714	0.291341	0.052002	0.181295
LINEX	0.094347	0.000208	0.056623	0.000046
95% CI	$(0.02541,\ 0.18522)$		$(0.019724,\ 0.095663)$	
95% HPD	$(0.022091,\ 0.174542)$		$(0.018905,\ 0.093007)$	

cle. A comprehensive theoretical framework was developed, encompassing the survival and hazard functions, modality structure, characteristic function, trigonometric moments, invariance behavior, and Rényi entropy, collectively demonstrating the analytical tractability and structural flexibility of the proposed model. An important contribution of this work is the development of characterization results for the WNPS distribution. Specifically, the distribution was characterized through a relationship between two truncated moments, as well as in terms of its hazard function. These characterizations provide alternative ways of identifying the distribution and contribute to a deeper theoretical understanding of its structural properties. Parameter estimation was addressed through ten classical methods. Among these, the MPS and AD estimators consistently delivered superior performance in terms of Bias, MSE, and MRE across all simulated configurations, establishing them as the preferred classical estimation strategies for the WNPS distribution. On the Bayesian front, estimators were derived under five loss functions i.e SELF, WSELF, MSELF, KLF, and LINEX via the Metropolis-Hastings algorithm with a Gamma prior. Across all sample sizes and parameter settings, the posterior risk declined steadily with increasing n, confirming estimator consistency. Notably, the LINEX loss yielded the smallest posterior risk, making it the recommended choice for Bayesian inference under this model. The practical utility of the WNPS distribution was validated through applications to two real circular datasets from ecological and wind direction studies. In both cases, the WNPS model achieved the lowest values across all considered information criteria, outperforming established competitors including the Wrapped Lindley, Wrapped Modified Lindley, and Wrapped XLindley distributions. MCMC convergence was thoroughly verified via trace plots, posterior density plots, and autocorrelation diagnostics for each dataset.

Taken together, the theoretical results, simulation evidence, and empirical findings position the WNPS distribution as a flexible, efficient, and practically viable model for circular data. Its simple one-parameter structure combined with strong goodness-of-fit performance makes it a compelling alternative for modeling angular and directional observations across a broad range of scientific applications.

References

Abramowitz, M. and Stegun, I. A. (1948). *Handbook of mathematical functions with formulas, graphs, and mathematical tables*, volume 55. US Government printing office.

Aguilar, G. A., Moala, F. A., and Cordeiro, G. M. (2019). Zero-truncated poisson exponentiated gamma distribution: application and estimation methods. *Journal of Statistical Theory and Practice*, 13(4):57.

Ahmad, Z., Mahmoudi, E., Hamedani, G., and Kharazmi, O. (2020). New methods to define heavy-tailed distributions with applications to insurance data. *Journal of Taibah University for Science*, 14(1):359–382.

Al-Meanazel, A. T. and Al-Khazaleh, A. M. (2021). Wrapped shanker distribution. *Ital. J. Pure Appl. Math*, 46:184–194.

Al-Mofleh, H. and Sen, S. (2019). The wrapped xgamma distribution for modeling circular data appearing in geological context. *arXiv preprint arXiv:1903.00177*.

Anderson, T. W. and Darling, D. A. (1952). Asymptotic theory of certain "goodness-of-fit" criteria based on stochastic processes. *The Annals of Mathematical Statistics*, 23(2):193–212.

Bhattacharjee, S., Ahmed, I., and Das, K. K. (2021). Wrapped two-parameter lindley distribution for modelling circular data. *Thailand Statistician*, 19(1):81–94.

Cheng, R. and Amin, N. (1983). Maximum product spacing estimation with applications to distributions. *Journal of the Royal Statistical Society: Series B (Methodological)*, 45(3):394–403.

Chesneau, C., Tomy, L., and Jose, M. (2021). Wrapped modified lindley distribution. *Journal of Statistics and Management Systems*, 24(5):1025–1040.

Choi, K. and Bulgren, W. (1968). An estimation procedure for mixtures of distributions. *Journal of the Royal Statistical Society Series B: Statistical Methodology*, 30(3):444–460.

Fisher, N. I. (1995). *Statistical analysis of circular data*. cambridge university press.

Gemeay, A. M. and Abd El-Bar, A. M. (2026). On wrapping a new version of lindley distribution for circular data analysis. *Environmental and Ecological Statistics*, pages 1–48.

Glänzel, W. (1987). A characterization theorem based on truncated moments and its application to some distribution families. *Mathematical statistics and probability theory*, Vol. B:75–84.

Glänzel, W. (1990). Some consequences of a characterization theorem based on truncated moments. *Statistics: A Journal of Theoretical and Applied Statistics*, 21(4):613–618.

Jammalamadaka, S. R. and Sengupta, A. (2001). *Topics in circular statistics*, volume 5. world scientific.

Joshi, S. and Jose, K. (2018). Wrapped lindley distribution. *Communications in Statistics-Theory and Methods*, 47(5):1013–1021.

Kao, J. H. K. (1958). A graphical estimation of mixed weibull parameters in life-testing of electron tubes. *Technometrics*, 1(4):389–407.

Kato, S. and Jones, M. (2013). An extended family of circular distributions related to wrapped cauchy distributions via brownian motion. *Bernoulli*, pages 154–171.

Keddali, M., Talhi, H., Meraou, M. A., and Slimani, A. (2026). The new polynomial single parameter distribution: Properties, bayesian and non-bayesian inference with real-data applications. *AppliedMath*, 6(4):60.

Mardia, K. V. and Jupp, P. E. (2009). *Directional statistics*. John Wiley & Sons.

Mastrantonio, G., Lasinio, G. J., Maruotti, A., and Calise, G. (2019). Invariance properties and statistical inference for circular data. *Statistica Sinica*, 29(1):67–80.

Nagano, Y., Yamaguchi, S., Fujita, Y., and Koyama, M. (2019). A wrapped normal distribution on hyperbolic space for gradient-based learning. In *International conference on machine learning*, pages 4693–4702.

Oliveira, M., Crujeiras, R. M., and Rodríguez-Casal, A. (2014). Npcirc: An r package for nonparametric circular methods. *Journal of Statistical Software*, 61(9):1–26.

Swain, J. J., Venkatraman, S., and Wilson, J. R. (1988). Least-squares estimation of distribution functions in johnson's translation system. *Journal of Statistical Computation and Simulation*, 29(4):271–297.

Torabi, H. (2008). A general method for estimating and hypotheses testing using spacings. *Journal of Statistical Theory and Applications*, 8(2):163–168.

Yilmaz, A. and Biçer, C. (2018). A new wrapped exponential distribution. *Mathematical Sciences*, 12(4):285–293.

Zinhom, E., Nassar, M., Radwan, S., and Elmasry, A. (2023). The wrapped xlindley distribution. *Environmental and Ecological Statistics*, 30(4):669–686.